Electrophysiological and pupillometric measures of inner retina function in nonproliferative diabetic retinopathy

Jason C. Park · Felix Y. Chau · Jennifer I. Lim · J. Jason McAnany

Abstract

Purpose To evaluate three measures of inner retina function, the pattern electroretinogram (pERG), the photopic negative response (PhNR), and the post-illumination pupil response (PIPR) in diabetics with and without nonproliferative diabetic retinopathy (NPDR).

Methods Fifteen non-diabetic control subjects and 45 type 2 diabetic subjects participated (15 have no clinically apparent retinopathy [NDR], 15 have mild NPDR, and 15 have moderate/severe NPDR). The pERG was elicited by a contrast-reversing checkerboard pattern, and the PhNR was measured in response to a full-field, long-wavelength flash presented against a short-wavelength adapting field. The PIPR was elicited by a full-field, 450 cd/m^2, short-wavelength flash. All responses were recorded and analyzed using conventional techniques. One-way ANOVAs were performed to compare the pERG, PhNR, and PIPR among the control and diabetic groups.

Results ANOVA indicated statistically significant differences among the control and diabetic subjects for all three measures. Holm-Sidak post hoc comparisons indicated small, nonsignificant reductions in the pERG (8%), PhNR (8%), and PIPR (10%) for the NDR group compared to the controls (all $p > 0.25$). In contrast, there were significant reductions in the pERG (35), PhNR (34%), and PIPR (30%) for the mild NPDR group compared to the controls (all $p < 0.01$). Likewise, there were significant reductions in the pERG (40%), PhNR (32%), and PIPR (32%) for the moderate/severe NPDR group compared to the controls (all $p < 0.01$).

Conclusion Abnormalities of the pERG, PhNR, and PIPR suggest inner retina neural dysfunction in diabetics who have clinically apparent vascular abnormalities. Taken together, these measures provide a noninvasive, objective approach to study neural dysfunction in these individuals.

Keywords Electroretinogram · Pattern electroretinogram · Photopic negative response · Pupillometry · Diabetic retinopathy

J. C. Park · F. Y. Chau · J. I. Lim · J. J. McAnany (✉)
Department of Ophthalmology and Visual Sciences,
University of Illinois at Chicago, 1855 W. Taylor St., MC/648, Chicago, IL 60612, USA
e-mail: jmcana1@uic.edu

J. J. McAnany
Department of Bioengineering, University of Illinois at Chicago, 851 South Morgan St., Chicago, IL 60607, USA

Introduction

Diabetic retinopathy (DR) continues to be the leading cause of vision loss among adults aged 20–74 years, affecting over 90 million individuals worldwide [1]. In addition to the well-described and widely studied

retinal vascular abnormalities in DR, there has recently been growing interest in the effects of diabetes on the function of the neural retina (see Adams and Bearse [2] and Lynch and Abramoff [3] for reviews). The structure and function of the inner retina in DR have been of particular interest, as the retinal ganglion cells (RGCs) appear to be susceptible to the effects of the disease. Since optical coherence tomography (OCT) became widely available, several studies have reported significantly reduced thickness of the RGC+ inner plexiform layer complex (RGC+) and of the retinal nerve fiber layer (RNFL) in diabetic patients who have no DR (NDR) or mild nonproliferative diabetic retinopathy (NPDR) [4–9].

In addition to structural abnormalities of the inner retina, functional deficits localized to the RGCs have been shown in DR, even in the early stages of the disease. For example, electrophysiological abnormalities in diabetic patients with NDR or mild NPDR have been reported [10, 11] using the pattern electroretinogram (pERG), which is primarily a measure of RGC function [12]. Additionally, the photopic negative response (PhNR) of the full-field ERG was shown to be reduced in amplitude in diabetics who have NPDR [13]; the PhNR is a slow negative component of the single-flash ERG that follows the b-wave and is largely mediated by RGCs [14]. Additional studies using single flash, flicker, and multifocal stimuli have shown electrophysiological changes in early-stage DR [15–21]. Although the pERG and PhNR have not been compared directly in diabetic subjects, the relationship between these measures has been evaluated in other visual disorders that affect the inner retina including glaucoma [22–24], autosomal dominant optic atrophy [25], and idiopathic intracranial hypertension [26]. These previous studies are generally consistent in showing both pERG and PhNR abnormalities in diseases that affect the inner retina and that the two measures are approximately equivalent in their ability to quantify inner retina dysfunction. This is not necessarily expected, as the measurement conditions under which these responses are obtained differ considerably: the pERG is driven by macular stimulation using an achromatic pattern stimulus of constant mean luminance, whereas the PhNR is typically a full-field measure elicited by a brief, long-wavelength pulse of light presented against a short-wavelength adapting field.

More recently, the post-illumination pupil response (PIPR), which was developed as an additional approach to evaluate RGC function more directly, has also been shown to be reduced in diabetics [27, 28]. The PIPR is characterized by a sustained pupillary constriction that follows the offset of a high-luminance, short-wavelength stimulus. This response is generally accepted to be an index of melanopsin photopigment activation and the function of intrinsically photosensitive retinal ganglion cells (ipRGCs). A study examining ipRGC gene expression in the human retina indicated reductions in ipRGC density in DR patients [29], which is consistent with the functional data from clinical studies [27, 28].

Thus, the pERG, PhNR, and PIPR all appear to be useful measures of RGC function in diabetes, but there is reason to suspect that these measures may not provide identical assessments of RGC function. Specifically, these tests target different classes of RGCs: the PIPR is mediated by ipRGCs that constitute a small fraction of the total RGC population ($\sim$ 1–2% of RGCs; [30]), whereas the PhNR and pERG target conventional (non-ipRGC) classes of RGCs. Additionally, as typically measured, the PhNR and PIPR are both full-field measures (ganzfeld stimulation) of RGC function that are sensitive to abnormalities of the peripheral retina, whereas the pERG is a macular test of RGC function (restricted area of stimulation). Furthermore, the adaptation conditions under which these measures are obtained also differ, as well as the spatiotemporal characteristics of the stimuli. Specifically, the PhNR and pERG are obtained under photopic conditions that are intended to minimize rod contributions to these measures. In contrast, the PIPR is obtained under dark-adapted conditions, but the response is believed to be largely driven by the melanopsin photopigment, with relatively little rod and cone contributions to the PIPR itself.

The primary goal of the present study was to compare RGC function measured with the pERG, PhNR, and PIPR to determine the extent to which these measures are altered in diabetic subjects with or without NPDR. We also sought to compare the relative deficits in each of these measures across disease severity, defined by conventional vascular markers. The results of this study may be of use in determining how these measures of inner retina neural function are related, for guiding the selection of outcome measures in future treatment trials that target retinal

neurodegeneration in DR, and for better understanding inner retina abnormalities in subjects with and without NPDR.

Methods

Subjects

Forty-five individuals diagnosed with type 2 diabetes mellitus (DM) were recruited from the Department of Ophthalmology and Visual Sciences at the University of Illinois at Chicago. Comprehensive histories were obtained from their medical records, and each subject was examined by a retina specialist, with particular attention to the optic nerve, retina, and its vasculature. The stage of NPDR was graded and the subjects were clinically classified as diabetic with no clinically apparent DR ($N = 15$), diabetic with mild NPDR ($N = 15$), or diabetic with moderate-severe NPDR ($N = 15$), according to the early treatment of diabetic retinopathy study (ETDRS) scale [31]. One eye (typically the right eye) was selected for testing. In rare cases in which the disease stage of the two eyes differed, the eye with the lower disease stage was tested. Ten of the NPDR subjects (three mild and seven moderate-severe) had a history of treatment with anti-VEGF and/or focal laser therapy in the tested eye. No subject had received panretinal photocoagulation. Of the 10 treated subjects, three moderate-severe NPDR subjects had clinically significant diabetic macular edema (DME) at the time of testing (ETDRS central subfield thickness greater than 305 μm [male] and 290 μm [female] as assessed by Heidelberg Spectralis SD-OCT [32, 33]).

Other than diabetes, no subject had systemic disease known to affect retinal function. Subjects who had sickle cell disease, high myopia, retinal vascular occlusions, hypertensive retinopathy, age-related macular degeneration, glaucoma, or other ocular disease were not recruited. Subject characteristics including age, sex, visual acuity, estimated diabetes duration, HbA1c percentage, and treatment history are provided in Table 1.

Fifteen visually normal, non-diabetic, control subjects also participated. The right eye of each control subject was selected for testing. All control subjects had best-corrected visual acuity of 0.06 log MAR (equivalent to approximately 20/23 Snellen acuity) or better, as assessed with the Lighthouse distance visual acuity chart, and normal letter contrast sensitivity as measured with a Pelli-Robson contrast sensitivity chart. The mean age of the control subjects did not differ significantly from that of the diabetic subjects ($F = 1.53$, $p = 0.22$). Ten of the control subjects and 18 of the diabetic subjects participated in a previous study of electrophysiological function in diabetes [28].

Pupillometry: apparatus, stimuli, procedure, and analysis

Stimuli for the pupil measurements were generated by and presented in a ColorDome desktop ganzfeld system (Diagnosys LLC, Lowell, MA) that we have used previously and described elsewhere [26, 34]. Prior to testing, the subject was dark-adapted for 10 min and a high-luminance (450 cd/m^2), 1-s duration, short-wavelength stimulus (dominant wavelength of 465 nm) was presented in the dark. In addition, pupil responses were elicited by a 450 cd/m^2,

Table 1 Subject characteristics

	Control ($N = 15$)	NDR ($N = 15$)	Mild NPDR ($N = 15$)	Mod-Sev NPDR ($N = 15$)
Age (yr)	52.2 ± 8.9	52.7 ± 6.8	55.1 ± 7.7	57.3 ± 4.3
Sex	6M 9F	2M 13F	7M 8F	6M 9F
Log MAR acuity	− 0.06 ± 0.06	0.01 ± 0.07	0.00 ± 0.05	0.03 ± 0.09
Disease duration (yr)		7.8 ± 5.9	15.5 ± 8.6	18.1 ± 10.3
HbA1c (%)		8.4 ± 2.3	8.4 ± 1.5	8.0 ± 1.4
Anti-VEGF Tx (N)		0	3	5
Focal laser Tx (N)		0	0	4

N number of subjects, yr years, M male and F female, MAR minimum angle of resolution, $HbA1c$ glycated hemoglobin, Tx treatment

1-s duration, long-wavelength stimulus (dominant wavelength of 642 nm) presented in the dark. The responses of the pupil to these stimuli were recorded from the test eye using an infrared camera system (ViewPoint EyeTracker, Arrington Research, Scottsdale, AZ), with the fellow eye patched. A minimum of 2 responses for each stimulus were obtained and averaged for analysis.

Data were analyzed offline using custom scripts programmed in MATLAB (MathWorks, Inc., Natick, MA, USA) as follows: first, a median filter with a 300-ms time window was applied to remove eye blinks. Long eye blinks could not be removed by the filter, and these artifacts were removed manually. The filtered pupil responses were then normalized by the median pupil size during the 1 s prior to each stimulus onset (prestimulus baseline pupil size). The relative pupillary light reflex (PLR) was defined as the ratio of the absolute pupil size (mm) to the baseline pupil size (mm), and the PIPR was defined as the median relative PLR between 5 and 7 s after stimulus offset [28, 34, 35].

pERG: apparatus, stimuli, procedure, and analysis

The pERG recordings generally conformed to ISCEV standards [12]. In brief, an achromatic checkerboard stimulus was displayed on a CRT monitor (ViewSonic model G90FB, Brea, CA, USA) at a refresh rate of 100 Hz. From the 57 cm test distance, each check subtended 0.9° and the total visual field size was 35° (width) × 25° (height). The photopic luminance for the light and dark checks was 82.4 cd/m^2 and 4.2 cd/m^2, respectively, yielding a Michelson contrast of 90%. The checkerboard contrast-reversed at 2 Hz (4 reversals per second). Subjects viewed the checkerboard stimulus through appropriate refractive correction with natural pupils.

The pERG was recorded with DTL electrodes; gold-cup electrodes were used as reference (ear) and ground (forehead). Amplifier bandpass settings were 0.6–100 Hz, and the sampling frequency was 2 kHz. A minimum of 150 responses that were free of blink artifacts were obtained and averaged for analysis. The P50 and N95 components of the pERG were selected manually, and the amplitude difference between these waveform components was used to define the pERG amplitude, per convention [12].

PhNR: apparatus, stimuli, procedure, and analysis

Flash stimuli for the PhNR studies were generated by and presented in a ColorDome desktop ganzfeld system (Diagnosys LLC, Lowell, MA), as described elsewhere [26, 36]. Prior to testing, the pupil of the tested eye was dilated (2.5% phenylephrine hydrochloride and 1% tropicamide drops) and the subject was light-adapted for 2 min to a uniform, short-wavelength, rod-suppressing field (465 nm; 12.5 cd/m^2). The stimulus consisted of a brief (4 ms), long-wavelength (642 nm) flash (3 cd-s/m^2).

ERGs were recorded with DTL electrodes; gold-cup electrodes were used as reference (ear) and ground (forehead). Amplifier bandpass settings were 0.3–300 Hz, and the sampling frequency was 2 kHz. A minimum of 5 responses that were free of eye blink and eye movement artifacts were obtained and averaged for analysis. The PhNR amplitude was defined as the difference between the mean baseline amplitude (10 ms before the stimulus was presented) and the mean amplitude within a 5-ms window centered at the trough of the response, consistent with conventional definitions [26, 36].

Statistical analysis

Data were analyzed using one-way analyses of variance (ANOVAs). Subject group (control, NDR, mild NPDR, and moderate-severe NPDR) was included as the main effect. Post hoc multiple comparisons between the subject groups were performed using the Holm-Sidak method. Receiver operating characteristic (ROC) curves were constructed to compare the control and diabetic groups based on response amplitude. From these curves, test sensitivity, specificity, and area under the curve (AUC) were derived. All statistical analyses were performed in SigmaPlot version 12.0 (SPSS; Chicago, IL, USA) with an alpha value of 0.05.

Results

Figure 1 shows the mean pERG (A), PhNR (B), and PLRs elicited by short-wavelength (C), and long-wavelength (D) stimuli. Mean traces are shown for the control subjects (black), NDR subjects (green), mild NPDR subjects (orange), and moderate-severe NPDR
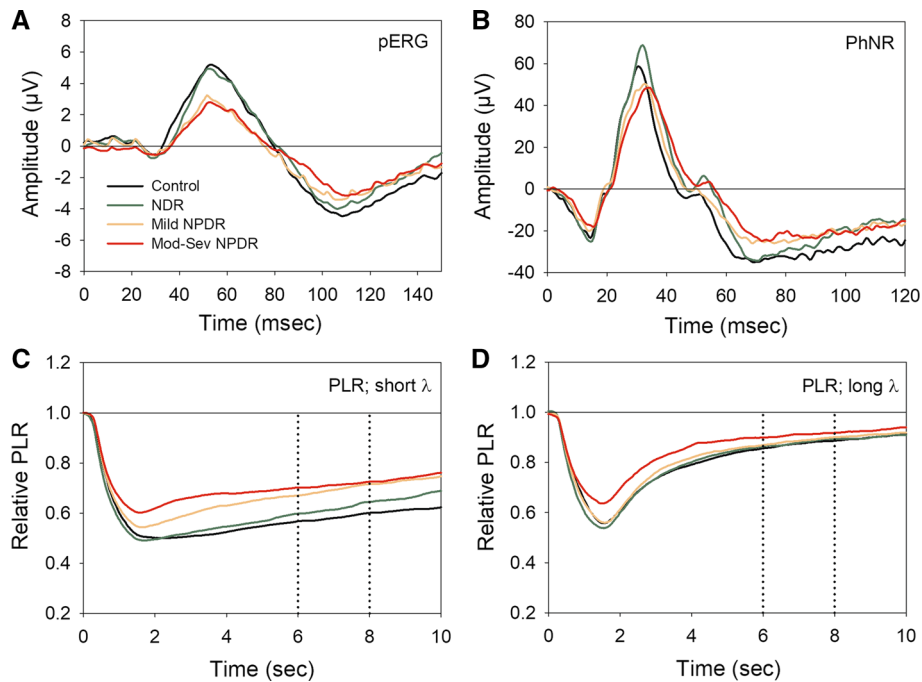
Fig. 1 Mean waveforms obtained for the pERG (**a**), PhNR (**b**), and PLR elicited by short-wavelength (**c**), and long-wavelength (**d**) stimuli. Each trace represents the mean response from the control subjects (black), NDR subjects (green), mild NPDR subjects (orange), and moderate-severe NPDR subjects (red). The vertical dashed lines in panels C and D mark the time window over which the PIPR is measured

subjects (red). The mean waveforms for the pERG and PhNR were similar for the NDR and control subjects. The mean response abnormality for the diabetics became apparent for the mild NPDR and moderate-severe NPDR subject groups (Fig. 1a, b). Likewise, the PLR elicited by short-wavelength light (C) was similar for the NDR and control subjects over the range in which the PIPR is measured (6–8 s following flash onset; dashed vertical lines). The response abnormality became apparent for the mild NPDR and moderate-severe NPDR subject groups. For the long-wavelength stimulus that was photopically matched to the short-wavelength stimulus (D), the PIPR measured 6–8 s after stimulus onset (dashed vertical lines) was absent for all four subject groups, as expected; the responses for the four subject groups were highly similar. Given the absence of the PIPR for the long-wavelength stimulus, these data were not analyzed further. The waveforms shown in Fig. 1 are intended to provide examples of the pattern of responses for the different subject groups, and data for individual subjects are discussed below.

Figure 2a shows the pERG amplitude for the four groups using the same color coding conventions as in Fig. 1. The gray boxes and horizontal bars show the range and mean of each group. It is apparent that the pERG amplitude tended to decrease across the subject groups, with the largest reductions observed for the moderate-severe NPDR subjects. A one-way ANOVA showed a significant pERG amplitude difference among the four subject groups ($F[3,59] = 15.22$, $p < 0.001$). Holm-Sidak pairwise comparisons indicated a statistically significant reduction in pERG amplitude for the mild NPDR group ($t = 4.86$, $p < 0.001$) and moderate-severe NPDR group ($t = 5.64$, $p < 0.001$) compared to the control group. However, the NDR group did not differ significantly from the control group ($t = 1.16$, $p = 0.25$). Thus, pERG amplitude was significantly reduced in both the mild NPDR group (35%) and moderate-severe NPDR group (40%), compared to the controls.

Figure 2b shows the PhNR amplitude for the four groups in the same manner as in panel A. The mean PhNR amplitude was slightly lower in the NDR group compared to the control group. The PhNR amplitude
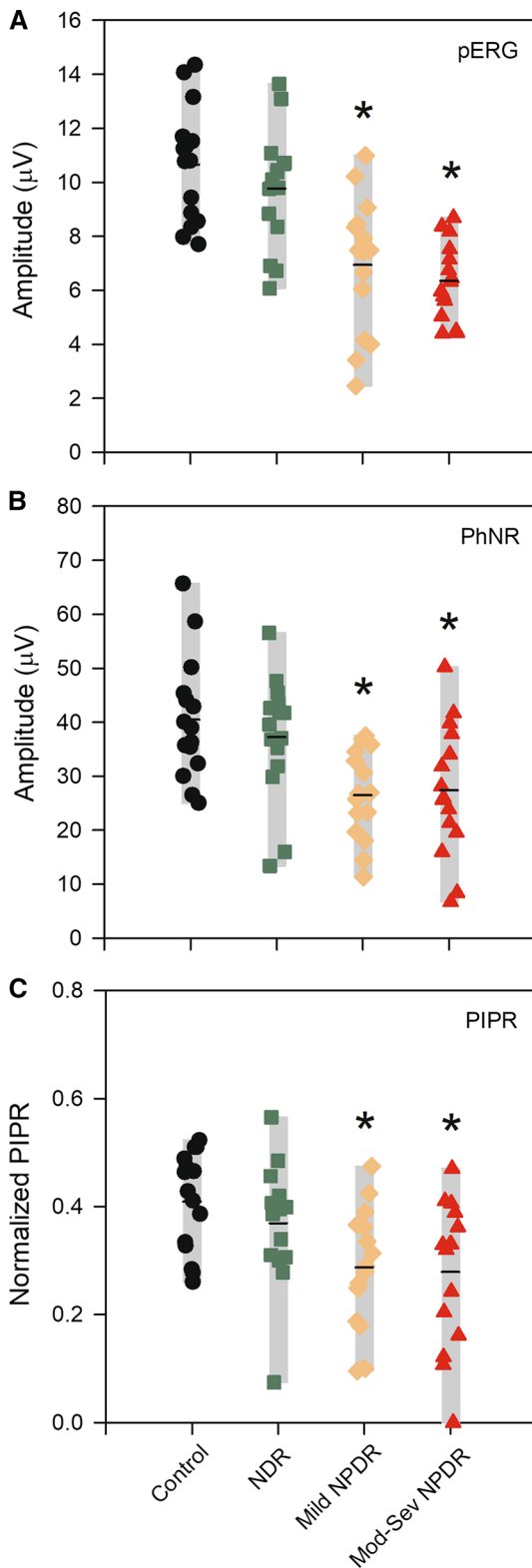
◀ **Fig. 2** Distribution of amplitudes for the pERG (**a**), PhNR (**b**), and PIPR (**c**). The gray regions indicate the range for each group and the horizontal bars show the mean of each group. Asterisks mark groups that differed significantly from the control group

reduction was more apparent for the mild and moderate-severe groups, as compared to the controls. One-way ANOVA indicated a significant difference among the PhNR amplitude for the four groups ($F[3,59] = 6.26$, $p < 0.001$). Holm-Sidak pairwise comparisons indicated a statistically significant reduction in PhNR amplitude for the mild NPDR group ($t = 3.52$, $p = 0.003$) and moderate-severe NPDR group ($t = 3.30$, $p = 0.003$) compared to the control group. The PhNR was reduced by 34% for the mild NPDR group and by 32% for the moderate-severe NPDR group compared to the controls. The NDR group, however, did not differ significantly from the control group ($t = 0.81$, $p = 0.42$).

Figure 2c shows the PIPR amplitudes for the four groups in the same manner as in panels A and B. The mean PIPR was slightly lower in the NDR group compared to the control group. The PIPR reduction was more apparent for the mild and moderate-severe groups, as compared to the controls. One-way ANOVA indicated significant differences in the PIPR among the four subject groups ($F[3,59] = 4.73$, $p = 0.005$). Holm-Sidak pairwise comparisons indicated a statistically significant reduction in the PIPR for the mild NPDR group ($t = 2.96$, $p = 0.01$) and moderate-severe NPDR group ($t = 3.15$, $p = 0.01$) compared to the control group. The PIPR was reduced by 30% for the mild NPDR group and by 32% for the moderate-severe NPDR group compared to the controls. The NDR group did not differ significantly from the control group ($t = 0.97$, $p = 0.34$). The data presented in Fig. 2a–c are summarized in Table 2. Data in Table 2 represent the mean and standard deviation (SD) for each measure for each group. Additionally, the associated p values (based on pairwise comparisons to the control group) for the three measures are provided.

As noted above, 10 subjects had a history of anti-VEGF and/or focal laser treatment. It is possible that current DME ($N = 3$), previous DME ($N = 10$), or treatment itself could have effects on retinal function [37]. To account for these potential effects, subjects with a history of treatment (including the three

Table 2 Summary of results

	Amplitude	SD	p value
pERG			
Control	10.66	2.15	0.253
NDR	9.77	2.15	
Mild NPDR	6.94	2.50	< 0.001
Mod-Sev NPDR	6.35	1.43	< 0.001
PhNR			
Control	40.50	11.27	0.420
NDR	37.29	11.25	
Mild NPDR	26.54	8.26	0.003
Mod-Sev NPDR	27.43	12.22	0.003
PIPR			
Control	0.41	0.09	0.337
NDR	0.37	0.11	
Mild NPDR	0.29	0.11	0.009
Mod-Sev NPDR	0.28	0.13	0.008

subjects who had DME at the time of testing) were excluded and the analyses described above were repeated. The results were not fundamentally different after excluding these 10 subjects, with one exception: the PIPR for the mild NPDR group became not significantly different from that of the controls. Specifically, one-way ANOVA showed a significant pERG amplitude difference among the four subject groups ($F[3,49] = 8.06$, $p < 0.001$). Holm-Sidak pairwise comparisons indicated a statistically significant reduction in pERG amplitude for the mild NPDR group ($t = 4.18$, $p < 0.001$) and moderate-severe NPDR group ($t = 3.78$, $p < 0.001$) compared to the control group. ANOVA also indicated significant differences among the four groups in PhNR amplitude ($F[3,49] = 4.29$, $p < 0.001$). Holm-Sidak pairwise comparisons indicated a statistically significant reduction in PhNR amplitude for the mild NPDR group ($t = 3.07$, $p = 0.011$) and moderate-severe NPDR group ($t = 2.57$, $p = 0.027$) compared to the control group. Likewise, one-way ANOVA indicated significant differences in the PIPR among the four subject groups ($F[3,49] = 2.83$, $p = 0.048$). Holm-Sidak pairwise comparisons indicated a statistically significant reduction in the PIPR for the moderate-severe NPDR group ($t = 2.33$, $p = 0.048$) compared to the control group, but not for the mild NPDR group ($t = 2.45$, $p = 0.054$). Thus, the pattern of results before and after

exclusion of treated subjects was generally the same. We note, however, that the sample size ($N = 3$) is underpowered to detect potential effects of current DME on these measures.

To compare the PhNR and pERG amplitude abnormalities, Fig. 3a plots the log PhNR amplitude loss versus the log pERG amplitude loss. In this figure, the data plotted on the *x*-axis and *y*-axis are normalized to the control mean. For example, in panel A, a value located at -0.5 (*x*-axis) and -0.5 (*y*-axis) would indicate a 0.5 log unit loss of pERG amplitude (*x*-axis) and a 0.5 log unit loss of PhNR amplitude (*y*-axis) relative to the control mean. The horizontal and vertical dashed lines mark the lower limit of the control PhNR (-0.19) and pERG (-0.13) amplitudes, respectively. All control subjects and 17 of the diabetic subjects fall in the upper right quadrant (normal pERG and PhNR). Diabetics who had reduced pERG amplitude but normal PhNR amplitude ($N = 14$) fall in the upper left quadrant, whereas diabetics who had a reduced PhNR amplitude but normal pERG amplitude ($N = 4$) fall in the lower right quadrant. Subjects who had reductions in both pERG and PhNR amplitude ($N = 10$) fall in the lower left quadrant.

Figure 3b compares the PhNR and PIPR losses by plotting the log PhNR amplitude loss versus the PIPR amplitude loss (other conventions are as in A). The horizontal and vertical dashed lines mark the lower limit of the control PhNR (-0.19) and PIPR (-0.15) amplitudes, respectively. All control subjects and 23 of the diabetic subjects fall in the upper right quadrant (both normal PIPR and PhNR). Diabetics who had a reduced PIPR but normal PhNR amplitude ($N = 8$) fall in the upper left quadrant, whereas diabetics who had a reduced PhNR amplitude but normal PIPR amplitude ($N = 9$) fall in the lower right quadrant. Subjects who had reductions in both PIPR and PhNR amplitude ($N = 5$) fall in the lower left quadrant.

Figure 3c compares pERG and PIPR losses in the same manner as panels A and B. The horizontal and vertical dashed lines mark the lower limit of the control pERG (-0.13) and PIPR (-0.15) amplitudes, respectively. All control subjects and 16 diabetic subjects fall in the upper right quadrant (both normal PIPR and pERG). Diabetics who had a reduced PIPR but normal pERG amplitude ($N = 5$) fall in the upper left quadrant, whereas diabetics who had a reduced pERG amplitude but a normal PIPR ($N = 16$)

Fig. 3 The relationship
between the PhNR
amplitude loss and the
pERG amplitude loss is
shown in **a**; relationship
between the PhNR
amplitude loss and the PIPR
loss is shown in **b**;
relationship between the
pERG amplitude loss and
the PIPR loss is shown in
c. All measurements have
been normalized to the
control mean, as discussed
in the text. Control subjects
are shown in black, NDR
subjects are shown in green,
mild NPDR subjects are
shown in orange and
moderate-severe NPDR
subjects are shown in red.
The vertical and horizontal
dashed lines mark the lower
limits of the control ranges,
as described in the text
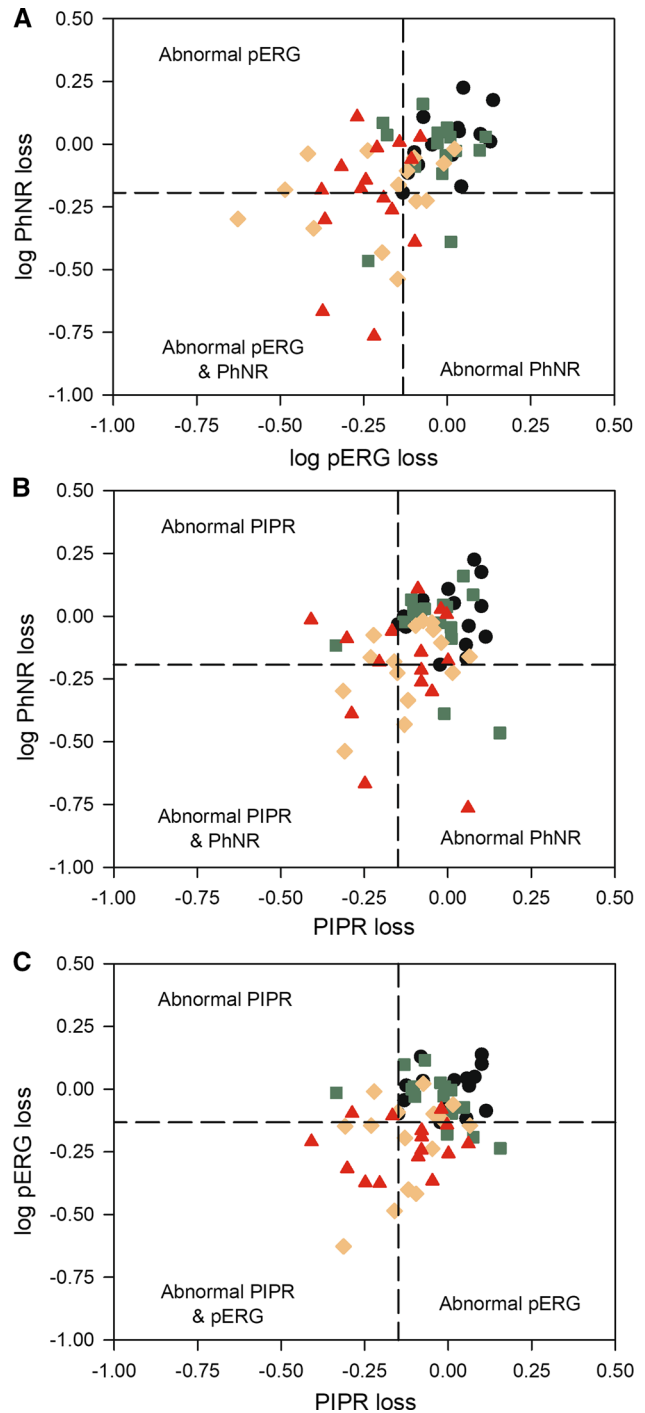
fall in the lower right quadrant. Subjects who had
reductions in both pERG and PIPR ($N = 8$) fall in the
lower left quadrant.

ROC curves were constructed as an additional
approach to compare the control and diabetic groups

based on response amplitude. Figure 4 plots test
sensitivity (proportion of diabetic subjects classified
as abnormal) as a function of 1-specificity (proportion
of control subjects classified as abnormal). The
optimal cutoff, sensitivity, specificity, and AUC based
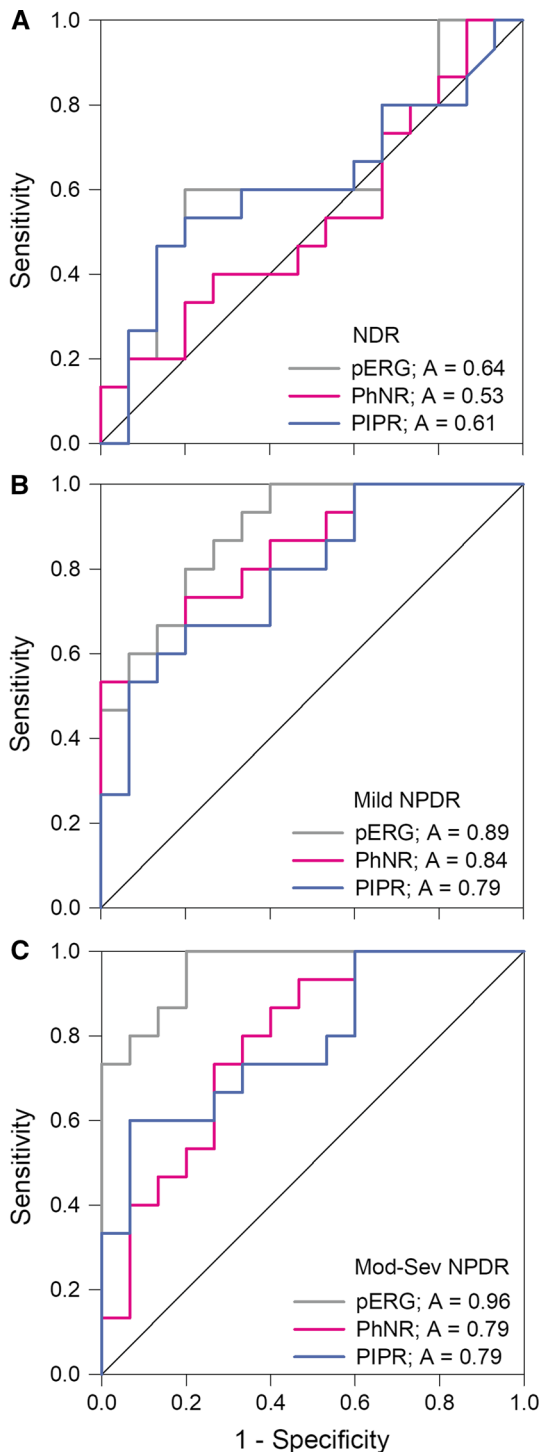
Fig. 4 Receiver operating characteristic curves for the NDR subjects (**a**), mild NPDR subjects (**b**), and moderate-severe NPDR subjects (**c**). The proportion of the DM subjects classified as abnormal (sensitivity) is plotted as a function of the proportion of the controls classified as abnormal (1-specificity; false positives). Data for the pERG are shown in gray, PhNR are shown in pink, and PIPR are shown in blue. The AUC values are provided in the inset. The optimal cutoff values, sensitivity, specificity, AUC, and corresponding *p* values derived from these plots are given in Table 3

≤ 0.64, $p \ge 0.21$). Relatively poor sensitivity, specificity, and a low AUC are expected based on the control and NDR data ranges shown in Fig. 2, which largely overlap. In comparison, the AUC values for the mild NPDR (B) and moderate-severe NPDR (C) groups were statistically significant for all three measures (all AUC ≥ 0.79, $p \le 0.01$). In general, the sensitivity values (0.60–1.00), specificity values (0.73–0.93), and AUC values (0.79–0.96) were approximately similar for the three measures for the mild and moderate-severe NPDR groups.

Discussion

The purpose of this study was to compare RGC deficits measured with the pERG, PhNR, and PIPR in a sample of diabetic subjects who have a range of disease severity. Our goal was to determine the extent to which these measures are altered in these individuals. The results showed that all three measures of RGC function were altered significantly in diabetic subjects who had mild or moderate-severe NPDR. In contrast, only nonsignificant trends of abnormality were apparent in diabetic subjects who had no clinically apparent retinopathy.

Overall, two-thirds of our sample of diabetic subjects had an abnormality on at least one measure. Approximately 53% had a pERG amplitude reduction, 29% had PhNR reduction, and 29% had a PIPR reduction (i.e., a value below the normal control range). Typically, when one measure was found to be abnormal, at least one other measure was found to be abnormal as well. For example, 92% of subjects who had a reduced PhNR also had a pERG and/or PIPR abnormality; only one patient had reduced PhNR amplitude with normal pERG and PIPR amplitude. Likewise, 77% of subjects who had a reduced PIPR

on these curves are shown in Table 3 for each subject group. For the NDR subjects (A), no measure was able to produce a statistically significant separation between the patients and the controls (all AUC

Table 3 Results of ROC analysis

	Cutoff	Sensitivity	Specificity	AUC	P value
pERG					
NDR	1.03	0.60	0.80	0.64	0.21
Mild NPDR	0.93	0.80	0.80	0.89	< 0.001
Mod-Sev NPDR	0.88	1.00	0.80	0.96	< 0.001
PhNR					
NDR	1.64	0.33	0.80	0.53	0.76
Mild NPDR	1.54	0.73	0.80	0.84	< 0.01
Mod-Sev NPDR	1.54	0.73	0.73	0.79	0.01
PIPR					
NDR	0.46	0.47	0.87	0.61	0.30
Mild NPDR	0.38	0.67	0.80	0.79	0.01
Mod-Sev NPDR	0.41	0.60	0.93	0.79	0.01

also had a pERG and/or PhNR abnormality. We did, however, observe subjects who had pERG amplitude loss with no PhNR or PIPR loss (37% of subjects). Nevertheless, subjects who had pERG amplitude loss also typically had either PhNR or PIPR abnormalities (63% of subjects).

ROC curves were constructed to determine the sensitivity, specificity, and AUC of the three measures for each patient group. In general, no measure was capable of significantly separating the NDR subjects from the control subjects (all AUC ≤ 0.64, $p > 0.21$). In contrast, all three measures had good diagnostic capability for the mild NPDR and the moderate-severe NPDR subject groups. The pERG tended to perform somewhat better than the PhNR or the PIPR in distinguishing the NPDR patients from the controls (i.e., larger AUC). Overall, there were modest differences in sensitivity, specificity, and AUC for the three measures, but the pERG did seem to be a somewhat better metric based on sensitivity, specificity, and AUC.

The approximate equivalence among the three tests suggests that they may be measuring a common effect of the disease on inner retina function. This is somewhat unexpected, given the marked differences in the spatiotemporal characteristics of the three tests, as discussed above. Furthermore, the PIPR is mediated by a small subset of RGCs (ipRGCs) that differs in many respects from the larger population of RGCs that are assessed with the pERG and PhNR. However, if diabetes similarly affects all RGC subtypes, then similar abnormalities obtained with the three measures might be expected. This appears to be the case in other

inner retina disorders that affect RGCs. In glaucoma, for example, the PIPR becomes more abnormal as the degree of structural impairment of the total RGC population increases [38–40]. Our group also showed that patients who have idiopathic intracranial hypertension (IIH) can have reduced PIPRs and the degree of abnormality is correlated with macular RGC volume [34]. The pERG and PhNR were also reduced in these individuals [26, 36], and the reductions were correlated with macular RGC volume. Despite these reports of RGC structure–function associations, it is important to consider that the pERG, PhNR, and PIPR are shaped by factors beyond the inner retina. For example, if diabetes affects the outer retina, then abnormalities in each of the functional measures may be expected, given that the outer retina is the source of RGC input. The PIPR, however, may be less affected by outer retina dysfunction, as this measure is largely driven by melanopsin activation of ipRGCs. Likewise, alterations in the vascular supply to the inner and/or outer retina may affect neurovascular coupling, which in turn might affect the pERG, PhNR, and PIPR. Thus, the three functional measures used in the present study are thought to arise from the inner retina, but potential contributions from other mechanisms (e.g., outer retina function, neurovascular coupling) cannot be ignored.

Given the similar abnormalities for each of the three measures, the choice of which test to use in future treatment trials or in clinical research may be based on convenience and available resources. That is, each measure has advantages and disadvantages for application to studying neural dysfunction in diabetes.

For example, the pERG is performed with natural pupils and without dark adaptation; the pERG also provided the largest AUC in our sample of subjects. The pERG, however, requires appropriate refractive correction, stable fixation, and equipment that is not available in many clinics. The PhNR does not require dark adaptation, refractive correction, or prolonged fixation, but this measure typically requires pupil dilation and is susceptible to eye movement artifacts and baseline drift [41]. Note that outer retina dysfunction could affect both the pERG and PhNR, which may complicate the interpretation of these measures. Finally, the PIPR is a more direct measure of ipRGC function, but this measure requires dark adaptation (10 min in the present study), specialized equipment (infrared videography), and is a measure of a unique, small population of RGCs.

In conclusion, the pERG, PhNR, and PIPR, three measures of RGC function, can be abnormal in diabetics who have at least some clinically apparent retinopathy, as defined by vascular abnormalities. Abnormalities in NPDR subjects recorded with these methodologies were approximately equivalent, indicating (1) the three measures may target similar underlying disease mechanisms and (2) the choice of which functional measure to use in future work can be guided by practical considerations.

Compliance with ethical standards

Conflict of interest All authors declare that there are no conflicts of interest.

Statements of human rights The study followed the tenets of the Declaration of Helsinki and was approved by a University of Illinois at Chicago institutional review board. All subjects provided written informed consent prior to participating.

Statement on the welfare of animals No animals were involved in this research.

Ethical approval All procedures performed in studies involving human participants were in accordance with the ethical standards of the institutional and/or national research committee and with the 1964 Helsinki declaration and its later amendments or comparable ethical standards. This article does not contain any studies with animals performed by any of the authors.

Informed consent Informed consent was obtained from all individual participants included in the study.

References

1. Lee R, Wong TY, Sabanayagam C (2015) Epidemiology of diabetic retinopathy, diabetic macular edema and related vision loss. Eye Vis 2:17. https://doi.org/10.1186/s40662-015-0026-2
2. Adams AJ, Bearse MA Jr (2012) Retinal neuropathy precedes vasculopathy in diabetes: a function-based opportunity for early treatment intervention? Clin Exp Optom 95(3):256–265. https://doi.org/10.1111/j.1444-0938.2012.00733.x
3. Lynch SK, Abramoff MD (2017) Diabetic retinopathy is a neurodegenerative disorder. Vision Res 139:101–107. https://doi.org/10.1016/j.visres.2017.03.003
4. Cabrera DeBuc D, Somfai GM (2010) Early detection of retinal thickness changes in diabetes using optical coherence tomography. Med Sci Monit Int Med J Exp Clin Res 16(3):MT15–MT21
5. Carpineto P, Toto L, Aloia R, Ciciarelli V, Borrelli E, Vitacolonna E, Di Nicola M, Di Antonio L, Mastropasqua R (2016) Neuroretinal alterations in the early stages of diabetic retinopathy in patients with type 2 diabetes mellitus. Eye 30(5):673–679. https://doi.org/10.1038/eye.2016.13
6. Lopes de Faria JM, Russ H, Costa VP (2002) Retinal nerve fibre layer loss in patients with type 1 diabetes mellitus without retinopathy. Br J Ophthalmol 86(7):725–728
7. van Dijk HW, Kok PH, Garvin M, Sonka M, Devries JH, Michels RP, van Velthoven ME, Schlingemann RO, Verbraak FD, Abramoff MD (2009) Selective loss of inner retinal layer thickness in type 1 diabetic patients with minimal diabetic retinopathy. Invest Ophthalmol Vis Sci 50(7):3404–3409. https://doi.org/10.1167/iovs.08-3143
8. van Dijk HW, Verbraak FD, Kok PH, Garvin MK, Sonka M, Lee K, Devries JH, Michels RP, van Velthoven ME, Schlingemann RO, Abramoff MD (2010) Decreased retinal ganglion cell layer thickness in patients with type 1 diabetes. Invest Ophthalmol Vis Sci 51(7):3660–3665. https://doi.org/10.1167/iovs.09-5041
9. van Dijk HW, Verbraak FD, Kok PH, Stehouwer M, Garvin MK, Sonka M, DeVries JH, Schlingemann RO, Abramoff MD (2012) Early neurodegeneration in the retina of type 2 diabetic patients. Invest Ophthalmol Vis Sci 53(6):2715–2719. https://doi.org/10.1167/iovs.11-8997
10. Ghirlanda G, Di Leo MA, Caputo S, Falsini B, Porciatti V, Marietti G, Greco AV (1991) Detection of inner retina dysfunction by steady-state focal electroretinogram pattern and flicker in early IDDM. Diabetes 40(9):1122–1127
11. Caputo S, Dileo MAS, Falsini B, Ghirlanda G, Porciatti V, Minella A, Greco AV (1990) Evidence for early impairment of macular function with pattern ERG in type-I diabetic-patients. Diabetes Care 13(4):412–418. https://doi.org/10.2337/diacare.13.4.412

12. Bach M, Brigell MG, Hawlina M, Holder GE, Johnson MA, McCulloch DL, Meigen T, Viswanathan S (2013) ISCEV standard for clinical pattern electroretinography (PERG): 2012 update. Doc Ophthalmol 126(1):1–7. https://doi.org/10.1007/s10633-012-9353-y

13. Chen H, Zhang M, Huang S, Wu D (2008) The photopic negative response of flash ERG in nonproliferative diabetic retinopathy. Doc Ophthalmol 117(2):129–135. https://doi.org/10.1007/s10633-008-9114-0

14. Frishman L, Sustar M, Kremers J, McAnany JJ, Sarossy M, Tzekov R, Viswanathan S (2018) ISCEV extended protocol for the photopic negative response (PhNR) of the full-field electroretinogram. Doc Ophthalmol 136(3):207–211. https://doi.org/10.1007/s10633-018-9638-x

15. McAnany JJ, Park JC (2018) Temporal frequency abnormalities in early-stage diabetic retinopathy assessed by electroretinography. Invest Ophthalmol Vis Sci 59(12):4871–4879. https://doi.org/10.1167/iovs.18-25199

16. McAnany JJ, Park JC, Chau FY, Leiderman YI, Lim JI, Blair NP (2018) Amplitude loss of the high-frequency flicker electroretinogram in early diabetic retinopathy. Retina. https://doi.org/10.1097/iae.0000000000002262

17. Pescosolido N, Barbato A, Stefanucci A, Buomprisco G (2015) Role of electrophysiology in the early diagnosis and follow-up of diabetic retinopathy. J Diabetes Res 2015:319692. https://doi.org/10.1155/2015/319692

18. Bearse MA Jr, Ozawa GY (2014) Multifocal electroretinography in diabetic retinopathy and diabetic macular edema. Curr DiabRep 14(9):526. https://doi.org/10.1007/s11892-014-0526-9

19. Holopigian K, Greenstein VC, Seiple W, Hood DC, Carr RE (1997) Evidence for photoreceptor changes in patients with diabetic retinopathy. Invest Ophthalmol Vis Sci 38(11):2355–2365

20. Tzekov R (2015) Full-field ERG in diabetic retinopathy: a screening tool? Graefes Arch Clin Exp Ophthalmol 253(7):987–988. https://doi.org/10.1007/s00417-015-3037-8

21. McAnany JJ, Park JC (2019) Cone photoreceptor dysfunction in early diabetic retinopathy: association between the activation phase of cone phototransduction and the flicker ERG. Invest Ophthalmol Vis Sci 60(1):64–72

22. Drasdo N, Aldebasi YH, Chiti Z, Mortlock KE, Morgan JE, North RV (2001) The s-cone PHNR and pattern ERG in primary open angle glaucoma. Invest Ophthalmol Vis Sci 42(6):1266–1272

23. North RV, Jones AL, Drasdo N, Wild JM, Morgan JE (2010) Electrophysiological evidence of early functional damage in glaucoma and ocular hypertension. Invest Ophthalmol Vis Sci 51(2):1216–1222. https://doi.org/10.1167/iovs.09-3409

24. Preiser D, Lagreze WA, Bach M, Poloschek CM (2013) Photopic negative response versus pattern electroretinogram in early glaucoma. Invest Ophthalmol Vis Sci 54(2):1182–1191. https://doi.org/10.1167/iovs.12-11201

25. Morny EK, Margrain TH, Binns AM, Votruba M (2015) Electrophysiological ON and OFF responses in autosomal dominant optic atrophy. Invest Ophthalmol Vis Sci 56(13):7629–7637. https://doi.org/10.1167/iovs.15-17951

26. Park JC, Moss HE, McAnany JJ (2018) Electroretinography in idiopathic intracranial hypertension: comparison of the pattern ERG and the photopic negative response. Doc Ophthalmol 136(1):45–55. https://doi.org/10.1007/s10633-017-9620-z

27. Feigl B, Zele AJ, Fader SM, Howes AN, Hughes CE, Jones KA, Jones R (2012) The post-illumination pupil response of melanopsin-expressing intrinsically photosensitive retinal ganglion cells in diabetes. Acta Ophthalmol 90(3):e230–e234. https://doi.org/10.1111/j.1755-3768.2011.02226.x

28. Park JC, Chen YF, Blair NP, Chau FY, Lim JI, Leiderman YI, Shahidi M, McAnany JJ (2017) Pupillary responses in non-proliferative diabetic retinopathy. Sci Rep 7:44987. https://doi.org/10.1038/srep44987

29. Obara EA, Hannibal J, Heegaard S, Fahrenkrug J (2017) Loss of melanopsin-expressing retinal ganglion cells in patients with diabetic retinopathy. Invest Ophthalmol Vis Sci 58(4):2187–2192. https://doi.org/10.1167/iovs.16-21168

30. Schmidt TM, Chen SK, Hattar S (2011) Intrinsically photosensitive retinal ganglion cells: many subtypes, diverse functions. Trends Neurosci 34(11):572–580. https://doi.org/10.1016/j.tins.2011.07.001

31. Davis MD, Fisher MR, Gangnon RE, Barton F, Aiello LM, Chew EY, Ferris FL 3rd, Knatterud GL (1998) Risk factors for high-risk proliferative diabetic retinopathy and severe visual loss: early treatment diabetic retinopathy study report #18. Invest Ophthalmol Vis Sci 39(2):233–252

32. Iglicki M, Busch C, Zur D, Okada M, Mariussi M, Chhablani JK, Cebeci Z, Fraser-Bell S, Chaikitmongkol V, Couturier A, Giancipoli E, Lupidi M, Rodriguez-Valdes PJ, Rehak M, Fung AT, Goldstein M, Loewenstein A (2019) Dexamethasone implant for diabetic macular edema in naive compared with refractory eyes: the international retina group real-Life 24-month multicenter study. The IRGREL-DEX Study. Retina 39(1):44–51. https://doi.org/10.1097/IAE.0000000000002196

33. Chalam KV, Bressler SB, Edwards AR, Berger BB, Bressler NM, Glassman AR, Grover S, Gupta SK, Nielsen JS, Diabetic Retinopathy Clinical Research N (2012) Retinal thickness in people with diabetes and minimal or no diabetic retinopathy: Heidelberg Spectralis optical coherence tomography. Invest Ophthalmol Vis Sci 53(13):8154–8161. https://doi.org/10.1167/iovs.12-10290

34. Park JC, Moss HE, McAnany JJ (2016) The pupillary light reflex in idiopathic intracranial hypertension. Invest Ophthalmol Vis Sci 57(1):23–29. https://doi.org/10.1167/iovs.15-18181

35. Adhikari P, Zele AJ, Feigl B (2015) The post-illumination pupil response (PIPR). Invest Ophthalmol Vis Sci 56(6):3838–3849. https://doi.org/10.1167/iovs.14-16233

36. Moss HE, Park JC, McAnany JJ (2015) The photopic negative response in idiopathic intracranial hypertension. Invest Ophthalmol Vis Sci 56(6):3709–3714. https://doi.org/10.1167/iovs.15-16586

37. Ozkiris A (2010) Pattern electroretinogram changes after intravitreal bevacizumab injection for diabetic macular edema. Doc Ophthalmol 120(3):243–250. https://doi.org/10.1007/s10633-010-9219-0

38. Duque-Chica GL, Gracitelli CPB, Moura ALA, Nagy BV, Vidal KS, Paranhos A Jr, Ventura DF (2018) Inner and outer retinal contributions to pupillary light response: correlation to functional and morphologic parameters in glaucoma.

J Glaucoma 27(8):723–732. https://doi.org/10.1097/IJG.0000000000001003

39. Adhikari P, Zele AJ, Thomas R, Feigl B (2016) Quadrant field pupillometry detects melanopsin dysfunction in glaucoma suspects and early glaucoma. Sci Rep 6:33373. https://doi.org/10.1038/srep33373

40. Gracitelli CP, Duque-Chica GL, Moura AL, Nagy BV, de Melo GR, Roizenblatt M, Borba PD, Teixeira SH, Ventura DF, Paranhos A Jr (2014) A positive association between intrinsically photosensitive retinal ganglion cells and retinal nerve fiber layer thinning in glaucoma. Invest Ophthalmol Vis Sci 55(12):7997–8005. https://doi.org/10.1167/iovs.14-15146

41. Tang J, Hui F, Coote M, Crowston JG, Hadoux X (2018) Baseline detrending for the photopic negative response. Transl Vis Sci Technol 7(5):9. https://doi.org/10.1167/tvst.7.5.9